

1 Title: PTP1B phosphatase puts a brake on iPSC-derived neutrophil motility and antimicrobial function
2 Short Title: Phosphatase signaling inhibits neutrophil function
3 Authors: Morgan A. Giese^{1,2}, David A. Bennin¹, Taylor J. Schoen^{1,3}, Ashley N. Peterson^{1,3}, Josh Brand^{4,5}, Ho
4 Sun Jung^{6,7}, Huy Q. Dinh⁵, Igor I. Slukvin^{6,7,8}, and Anna Huttenlocher^{1,9,*}

5

6 ¹Department of Medical Microbiology and Immunology, University of Wisconsin-Madison, Madison, WI,
7 USA.

8 ²Cellular and Molecular Biology Graduate Program, University of Wisconsin-Madison, Madison, WI, USA.

9 ³Comparative Biomedical Sciences Graduate Program, University of Wisconsin-Madison, Madison, WI,
10 USA.

11 ⁴Cell and Molecular Pathology Graduate Program, University of Wisconsin-Madison, Madison, WI, USA.

12 ⁵Department of Oncology, McArdle Laboratory for Cancer Research, School of Medicine and Public
13 Health, University of Wisconsin-Madison, Madison, WI, USA.

14 ⁶Wisconsin National Primate Research Center, University of Wisconsin, Madison, WI, USA.

15 ⁷Department of Cell and Regenerative Biology, University of Wisconsin School of Medicine and Public
16 Health, Madison, WI, USA.

17 ⁸Department of Pathology and Laboratory Medicine, University of Wisconsin, Madison, WI, USA.

18 ⁹Department of Pediatrics, University of Wisconsin-Madison, Madison, WI, USA.

19 *Corresponding author: huttenlocher@wisc.edu (AH)

20 Text word count: 4000

21 Abstract word count: 172

22 Figure count: 5

23 Reference count: 44

24

25 Key points:

26 Deletion of PTP1B increases iPSC-derived neutrophil intracellular signaling to improve motility and
27 phagocytosis.

28 Deletion of PTP1B enhances iPSC-derived neutrophil swarming response and ability to inhibit fungal
29 growth.

30

31

32

33

34

35

36

37

38

39 **Abstract**

40 Neutrophils are rapidly recruited to sites of infection and are critical for pathogen clearance.
41 Neutropenic patients are at high risk for fungal and bacterial infections and can benefit from
42 granulocyte transfusion therapy. Human induced pluripotent stem cells (iPSCs) could provide a robust
43 source of neutrophil-like cells for infusion as they can be generated in large quantities and do not
44 require a donor. However, dampened intracellular signaling limits their cellular activation and response.
45 Here, we show that we can engineer iPSC-derived neutrophils (iNeutrophils) for enhanced motility and
46 anti-microbial functions. Deletion of the PTP1B phosphatase increased iNeutrophil PI3K and ERK
47 signaling and was associated with increased F-actin polymerization, cell migration and phagocytosis.
48 PTP1B deletion also increased production of inflammatory cytokines, including the neutrophil
49 chemoattractant IL-8. Furthermore, PTP1B-KO iNeutrophils displayed a highly activated morphology and
50 were more responsive to the fungal pathogen *Aspergillus fumigatus*. KO iNeutrophils efficiently
51 migrated to and swarmed hyphae resulting in inhibition of fungal growth. Taken together, deletion of
52 the PTP1B phosphatase removes the “brakes” on iPSC-derived intracellular signaling and neutrophil
53 function.

54

55 **Introduction**

56 Neutrophils are highly motile cells and as first responders of innate immunity are critical for
57 clearing bacterial and fungal infections. They exhibit an arsenal of anti-microbial functions, including
58 production of reactive oxygen species (ROS), release of neutrophil extracellular traps (NETs), and
59 phagocytosis of pathogens. Patients who have received bone marrow transplant or chemotherapy can
60 become neutropenic, leading to higher rates of mortality due to increased susceptibility to bacterial and
61 fungal infections¹. Alongside administration of antifungals or antibiotics, granulocyte transfusion
62 therapy (GTX) can be utilized to improve patient outcomes. However, success of GTX has suffered from
63 donor yield, as well as the short lifespan and functional capacity of primary human neutrophils ex vivo².
64 Thus, there is need for identification of alternative sources of infusible neutrophils.

65 Induced pluripotent stem cells (iPSC)-derived neutrophils (iNeutrophils) have emerged as a
66 promising option for treating neutropenic patients as no donor is required, the cells are genetically
67 malleable, and can be generated in large numbers. iNeutrophils have been shown to migrate effectively
68 and exert many neutrophil antimicrobial functions³⁻⁶. However, their functional capacity is often lower
69 than primary human neutrophils³⁻⁶. iNeutrophils were shown to have dampened activation of
70 intracellular signaling pathways, such as phospho-AKT, that limit functions including migration,
71 phagocytosis and NETosis⁶. Thus, inhibitory signaling pathways may prevent full activation and
72 response. Methods to activate intracellular signaling pathways may improve iNeutrophil function for
73 future use as a clinical therapy for neutropenic patients. Furthermore, iNeutrophils can be a valuable
74 tool to study the molecular signaling pathways that regulate neutrophil migration and antimicrobial
75 function.

76 Here, we show that we can engineer iPSC-derived neutrophils to enhance cellular activation,
77 motility and antimicrobial response. Protein Tyrosine Phosphatases such as PTP1B negatively regulate
78 many signaling pathways involved in neutrophil function⁷. Deletion of the PTP1B phosphatase increased
79 iNeutrophil PI3K and ERK signaling leading to increased F-actin polymerization, cell migration and
80 phagocytosis. PTP1B-KO iNeutrophils produced higher levels of inflammatory chemokines, including the
81 neutrophil chemoattractant IL-8. Furthermore, PTP1B-KO iNeutrophils displayed a highly activated
82 morphology in the presence of the fungal pathogen *Aspergillus fumigatus*, efficiently migrated to and

83 swarmed hyphae, and limited fungal growth. Thus, deletion of the PTP1B phosphatase removes the
84 “brakes” on iPSC-derived intracellular signaling and neutrophil function.

85

86 **Methods**

87 **Stem Cell Culture and Neutrophil Differentiation**

88 Neutrophils were differentiated from the bone marrow-derived IISH2i-BM9 cell line (WiCell)⁸. hiPSCs
89 were cultured on Matrigel-coated plates in mTeSR-Plus medium. To induce hemogenic endothelium,
90 hiPSCs are transfected with *ETV2* mmRNA. One day following transfection, media was changed to
91 StemLinell with VEGF-165 and FGF to induce differentiation into hemogenic endothelial cells. After two
92 days, media was changed to StemLinell supplemented with FGF2, GM-CSF, and UM171 to generate
93 common myeloid progenitors (CMPs). On days 8-10, floating cells were gently harvested and cultured in
94 StemSpan SFEM II supplemented with GlutaMAX, ExCyte, G-CSF and Am580 to promote terminal
95 neutrophil differentiation. Floating neutrophils were harvested after another 8-10 days.

96

97 **Generation of PTP1B^{-/-} BM9iPSCs**

98 Cells were nucleofected with Cas9 protein and two guide RNAs targeting Exon 3 of *PTPN1*. Individual
99 colonies were picked and expanded. To confirm biallelic mutation, clones were screened by PCR for the
100 acquisition of a 67 bp deletion. Loss of protein expression was verified by western blot.

101

102 **Human Neutrophil Isolation**

103 Human blood was obtained from volunteering donors with informed written consent through a protocol
104 that was approved by the Internal Review Board of the University of Wisconsin-Madison. Neutrophils
105 were isolated using MACSxpress negative antibody selection kit and purified with the MACSxpress
106 erythrocyte depletion kit.

107

108 **Flow Cytometry**

109 Neutrophils were stained (**Supplementary Table 1**), fixed and acquired on an Aurora Cytometer.
110 Myeloid cells were identified by CD11b+ expression and neutrophils were identified by CD15+ or
111 CD15+CD16+ expression. Monocytes were identified as CD14+. Data were analyzed using FlowJo
112 Software (v10.8.1).

113

114 *Flow cytometry analysis in R using Cytoflow*

115 Exported .fcs files were analyzed with *prepData* function from Cytoflow (v1.14.0) pipeline⁹. Data
116 transformation was calculated for all fluorescent parameter using an *arcsinh* normalization and a
117 cofactor of 3000. Transformed data were plotted using a smoothed density function using *ggplot2* to
118 show proportion of cell types over the range of expression values.

119

120 **Presto Blue Viability**

121 Cells were plated and incubated at 37°C. For each timepoint, Presto Blue HS was added and incubated
122 for 30 minutes before reading fluorescence at 560/590 nm in a microplate reader.

123

124 **Western Blot Cell Signaling**

125 Cells were stimulated with 1uM fMLP for 3 minutes then collected in lysis buffer with protease and
126 phosphatase inhibitors. Cells were sonicated and clarified by centrifugation. Protein concentrations
127 were determined and immunoblotting of cell lysates was performed (**Supplementary Table 2**) and blots
128 were imaged with an infrared imaging system.

129

130

131

132 **Chemotaxis**

133 Chemotaxis was assessed using a microfluidic device ¹⁰. Polydimethylsiloxane (PDMS) devices were
134 adhered to glass coverslips and coated with fibrinogen. Calcein stained cells were added before addition
135 of fMLP. Cells were imaged every 30 seconds for 45–90 min on an inverted fluorescent microscope with
136 a 10× objective and an automated stage. Cell tracking analysis was done using JEX software ¹¹.

137

138 **Immunofluorescent imaging**

139 Cells were stimulated in an fMLP bath for 30 minutes at 37°C, then fixed, permeabilized, and incubated
140 with Rhodamine-phalloidin overnight at 4°C. Coverslips were counterstained with Hoechst 33342 and
141 imaged on an upright Laser Scanning Confocal Microscope equipped with a motorized stage. Images
142 were acquired with a 60× oil, NA 1.40 objective and processed in ZenBlue software. Maximum intensity
143 projections were generated and integrated density of the actin channel was quantified using ImageJ.

144

145 **Phagocytosis**

146 pHrodo™ Green *E. coli* BioParticles were opsonized with 30% pooled human serum and incubated with
147 iNeutrophils (100:1 MOI) for 1 hour at 37°C. Reaction was stopped by addition of ice cold PBS. Cells were
148 stained for flow cytometry (**Supplementary Table 1**) on ice, then fixed before analysis using an Aurora
149 Cytometer.

150

151 **NETosis and Intracellular ROS**

152 For NETosis, cells were stimulated with PMA and incubated for 4 hours at 37°C before endpoint addition
153 of Sytox Green. For ROS assay, DHR123 probe was added before PMA and plate was read every 15
154 minutes after stimulation. NETosis (500/528nm) and ROS (485/535nm) fluorescence was quantified
155 using a microplate reader.

156

157 **Real Time qPCR**

158 Cells were stimulated with 200ng/mL *E. coli* LPS for 2 hours at 37°C, then collected in Trizol for RNA
159 isolation. cDNA was synthesized and used as the template for quantitative PCR (qPCR) (**Supplementary**
160 **Table 3**). Data were normalized to *ef1a* within each sample using the $\Delta\Delta Cq$ method ¹². Fold-change
161 represents the change in cytokine expression over the unstimulated WT sample.

162

163 **Inflammatory Cytokine and LTB4 ELISA**

164 For inflammatory cytokines IL-8, IL-1beta, IL-6 and TNFa, iNeutrophils were stimulated with 200ng/mL *E.*
165 *coli* LPS or 10ug/mL Zymosan for 4 hours at 37°C. For LTB4, iNeutrophils were stimulated with 1uM fMLP
166 for 5 or 30 minutes at 37°C. Supernatants were collected, aliquoted and frozen at -80°C until
167 quantification by ELISA.

168

169 **Fungal co-culture imaging**

170 *Aspergillus fumigatus* (CEA10) was grown as previously described ¹³. For imaging experiments, *A.*
171 *fumigatus* were incubated until germling stage (37°C for 8 hours). GMM media was removed and
172 replaced with neutrophil suspension (MOI 150:1). Images were taken every 3 minutes on an inverted
173 fluorescent microscope with a 20× objective and an automated stage at 37°C with 5% CO₂. Videos were
174 compiled using ImageJ software.

175

176 *Image Analysis*

177 iNeutrophil *circularity* and cluster size was quantified by outlining individual cells or clusters using the
178 Polygon selection tool (ImageJ). A cluster was identified as a tightly formed group of at least 5
179 iNeutrophils attached to *A. fumigatus*. Hyphal length was measured using the segmented line feature
180 (ImageJ).

181

182 Statistical Analysis

183 All experiments and statistical analyses represent at least three independent replicates. Analysis
184 of chemotactic index and cell velocity was performed using unpaired Student's t-test. Analysis of
185 receptor expression by flow cytometry, phagocytosis, qPCR gene expression and ELISA was performed
186 using paired Student's t-test. Analysis of Presto Blue viability, ROS production, and percent of clustered
187 germlings was performed using simple linear regression and the p value was calculated by comparing
188 the slope of each line. Analysis of cluster size over time was performed by calculating the area under the
189 curve (AUC) for each replicate and then determining the p value using a paired Student's t-test. Analysis
190 of NETosis and phospho-signaling was performed using One Sample t-test. Above analyses were
191 conducted using GraphPad Prism (v9). Integrated Density of F actin, circularity, and hyphal length
192 analysis represent least-squared adjusted means±standard error of the mean (LSmeans±s.e.m.) and
193 were compared using ANOVA with Tukey's multiple comparisons (RStudio).

194

195 Results

196 Generation of PTP1B-KO iPSC-derived neutrophils

197 To increase activation of intracellular signaling pathways in iPSC-derived neutrophils, we deleted
198 the protein tyrosine phosphatase 1B (PTP1B), encoded by *PTPN1*, using CRISPR/Cas9 mediated gene
199 mutation at the iPSC-stage (Figure 1A). We generated clonal cell lines with biallelic deletion of *PTPN1*
200 (Supplementary Figure 1A), and then differentiated these cells into human iPSC-derived neutrophils
201 using serum-and feeder-free conditions, following published protocols^{5,8} (Figure 1B). Loss of PTP1B
202 protein expression was confirmed both at the stem cell stage and after neutrophil differentiation by
203 western blot (Supplementary Figure 1B, Figure 1C). Morphological characteristics of differentiated
204 neutrophils were examined by cytopsin, confirming the presence of hyper-segmented nuclei (Figure 1D).

205 Further validation of neutrophil differentiation was completed by staining for neutrophil surface
206 receptors. As previously reported, almost all iNeutrophils expressed the common myeloid marker
207 CD11b, but less than 20% expressed the canonical human neutrophil marker CD66b or mature
208 neutrophil marker CD10. However, the majority of iNeutrophils expressed primary blood and mature
209 neutrophil markers CD15 and CD16 (Figure 1E, F)^{3,5}. While deletion of PTP1B resulted in a lower
210 proportion of fully mature CD16+ neutrophils, the majority of PTP1B-KO cells still expressed CD15
211 (Figure 1E). PTP1B has been shown to modify murine myelopoiesis by negatively regulating monocyte
212 differentiation¹⁴, however, we did not find a significant increase in CD14+ monocytes upon PTP1B
213 deletion in human iPSCs (Figure 1E). Our data indicate that deletion of PTP1B at the stem cell stage still
214 allows for neutrophil differentiation.

215 A limitation of primary human peripheral blood (PB) neutrophils is their short life span ex vivo.
216 To determine if the lifespan of iNeutrophils is longer than that of PB neutrophils, we evaluated the
217 longevity of these cells in culture. PB neutrophils exhibited less than 30% viability at 3 days, whereas
218 iNeutrophils were 50% viable after 5 days, with no difference between WT and PTP1B-KO cells (Figure
219 1G). The lower maturation level of our iNeutrophils may explain the longer lifespan of these cells
220 compared to fully matured PB neutrophils.

221

222 **Deletion of PTP1B promotes intracellular signaling, motility and actin polymerization**

223 Previously we and others have reported that PTP1B regulates the actin cytoskeleton and inhibits
224 migration of cancer cells ^{15,16}. To determine if PTP1B also regulates signaling and motility of human
225 iNeutrophils, we first quantified phospho-signaling induced by the bacterial formylated peptide fMLP.
226 PTP1B negatively regulates MAPK and PI3K signaling pathways ¹⁷. PTP1B-KO iNeutrophils showed
227 increased phosphorylation of ERK1/2, AKT, and HS1 compared to WT iNeutrophils (Figure 2A, B). HS1 is
228 an actin binding protein that regulates actin dynamics during cell migration via its interaction with the
229 Arp2/3 complex. Enhanced phosphorylation of HS1 is correlated with efficient directed neutrophil
230 migration ¹⁸. Using a previously published microfluidic device ¹⁹, we conducted short term live imaging of
231 neutrophil migration in response to the chemoattractant fMLP. PTP1B-KO iNeutrophils displayed
232 enhanced motility with higher chemotactic index and velocity compared to WT cells (Figure 2C).
233 Representative cell tracks show increased directed migration of PTP1B-KO iNeutrophils (Figure 2D).
234 During migration, actin is polymerized at the leading edge to drive pseudopod formation ²⁰. As elevated
235 p-HS1 may increase actin polymerization to promote PTP1B-KO iNeutrophils chemotaxis, we next
236 imaged F-actin polymerization in iNeutrophils after stimulation in an fMLP bath. PTP1B-KO cells
237 displayed increased density of total F-actin compared to WT cells by immunofluorescent staining (Figure
238 2E, F). Thus, deletion of the PTP1B phosphatase increases intracellular ERK and PI3K signaling and the
239 motility of iNeutrophils.

240

241 **Deletion of PTP1B improves neutrophil phagocytosis but decreases production of ROS and NETs**

242 Increased intracellular phospho-signaling may promote neutrophil antimicrobial functions,
243 including the ability to phagocytose microbes ⁷. Furthermore, phagocytosis is mediated by actin
244 contraction to form the phagosome ²¹, and thus, we hypothesized this function may be enhanced in
245 PTP1B-KO iNeutrophils. We quantified phagocytosis of *E. coli* coated beads by flow cytometry and found
246 a significant increase in phagocytosis by CD15+ PTP1B-KO iNeutrophils (Figure 3A). This effect was
247 heightened when gating on CD15+ CD16+ mature neutrophils with 80% of PTP1B-KO iNeutrophils
248 phagocytosing and acidifying *E. coli* coated beads, whereas less than 50% of WT cells had after 1 hour.

249 Following phagocytosis, neutrophils can kill pathogens by production of intracellular reactive
250 oxygen species (ROS). While PTP1B-KO iNeutrophils produced lower levels of ROS than WT cells, PTP1B-
251 KO iNeutrophils were still capable of producing ROS at high levels upon PMA stimulation (Figure 3B). It is
252 likely the PTP1B-KO iNeutrophils produce levels similar to that of human PB neutrophils (Supplementary
253 Figure 2A). Another antimicrobial mechanism is the release of neutrophil extracellular traps (NETs).
254 Upon PMA stimulation, we found that PTP1B-KO iNeutrophils make fewer NETs (Figure 2E). ROS
255 production is necessary for NET release ²², thus, the decreased production of NETs correlates with the
256 decrease in ROS we observed in PTP1B-KO iNeutrophils.

257

258 **Deletion of PTP1B increases inflammatory cytokine production**

259 Upon migrating to sites of infection, neutrophils can produce inflammatory cytokines to further
260 recruit and promote the innate and adaptive immune response. IL-8 is a strong neutrophil
261 chemoattractant and activating factor. *CXCL8* transcripts were increased both basally and upon LPS
262 stimulation in PTP1B-KO iNeutrophils (Supplemental Figure 3A), indicating that PTP1B negatively
263 regulates IL-8 expression. We confirmed increased production at the protein level with both LPS and
264 Zymosan stimulation (Figure 4A). Increased production of IL-8 may contribute to enhanced iNeutrophil
265 activation and chemotactic response during bacterial or fungal infection. We also found differential
266 production of the inflammatory cytokines TNF α , IL1 β and IL-6. PTP1B-KO iNeutrophils showed
267 comparable levels of *IL1B* at the basal level (Supp. Figure 3B), but significantly increased protein
268 secretion upon stimulation (Figure 4B). Additionally, PTP1B-KO iNeutrophils showed elevated secretion

269 of IL-6 and TNF α after stimulation (Supplemental Figure 3C, D, Figure 4C, D). Taken together these
270 findings suggest that PTP1B negatively regulates inflammatory cytokine production.

271 To determine if increased cytokine production by PTP1B-KO iNeutrophils is due to altered
272 expression of pathogen recognition receptors (PRRs), rather than increased intracellular signaling, we
273 quantified expression of Dectin-1, TLR2, and TLR4 on WT and KO iNeutrophils. Zymosan is recognized by
274 Dectin-1 and TLR2, whereas LPS is primarily recognized by TLR4²³. We found similar levels of expression
275 of these receptors on WT and KO cells, thus the increase in inflammatory cytokine production is not due
276 to differences in PRR expression (Supplementary Figure 3E). Our findings show that PTP1B-KO cells are
277 more responsive to microbial induced production of inflammatory cytokines compared to WT
278 iNeutrophils.

279 **Deletion of PTP1B increases iNeutrophil swarming and inhibition of fungal growth**

280 After evaluating the effect of PTP1B deletion on specific neutrophil functions, we next wanted to
281 determine if PTP1B expression affects iNeutrophil response to the live fungal pathogen *Aspergillus*
282 *fumigatus*. We co-cultured iNeutrophils with *A. fumigatus* at the germling stage and then live imaged
283 iNeutrophil-fungal interactions over the course of 8 hours (Figure 5A). We noticed a stark difference in
284 the morphology of WT vs PTP1B-KO iNeutrophils in the presence of *A. fumigatus*. During co-incubation,
285 KO iNeutrophils displayed an elongated cell shape indicative of cell activation (Figure 5B). Specifically,
286 PTP1B-KO iNeutrophils showed significantly decreased circularity in the presence of *A. fumigatus* (Figure
287 5C). In contrast, the majority of WT cells remained maintained a round morphology, even after 4 hours
288 (Figure 5B, C). Limited activation of WT iNeutrophils in response to *A. fumigatus* is likely not due to
289 decreased recognition, as we saw no difference in Dectin-1 expression (Supplementary Figure 3E) but
290 may be due to dampened signaling mediated by PTP1B.

291 We next analyzed iNeutrophil motility in response to *A. fumigatus* fungal growth. We found that
292 PTP1B-KO iNeutrophils were highly migratory and rapidly recruited and swarmed *A. fumigatus* (Video
293 S1). In contrast, WT iNeutrophils showed a delayed response with fewer cells migrating and physically
294 interacting with germlings or hyphae (Video S2, S3). Furthermore, we observed many instances of
295 PTP1B-KO iNeutrophils phagocytosing germlings that led to enhanced neutrophil recruitment and
296 swarming (Figure 5D and Video S4, S5). PTP1B-KO iNeutrophils formed tight clusters around *A.*
297 *fumigatus* significantly faster and larger in size than WT cells (Figure 5E, F). Neutrophil swarming is
298 mediated by release of LTB4²⁴, therefore, increased swarming by PTP1B-KO iNeutrophils could indicate
299 increased production of LTB4 or expression of its receptor BLT1R. We found that almost 100% of WT and
300 KO iNeutrophils expressed BLT1R but found no difference in the level of expression between genotypes
301 (Supplementary Figure 4A, B). We quantified LTB4 release upon fMLP stimulation and saw no significant
302 difference between WT and KO cells (Supplementary Figure 4C). Thus, swarming by PTP1B-KO
303 iNeutrophils is likely due to enhanced cell activation that leads to migration and physical interaction
304 with *A. fumigatus*.

305 Lastly, we wanted to determine if heightened PTP1B-KO iNeutrophil recruitment and swarming
306 of *A. fumigatus* limited fungal growth. We quantified the hyphal length for each germling at 0 and 4
307 hours of co-incubation. After 4 hours, hyphal growth was significantly decreased when cultured with
308 PTP1B-KO neutrophils, compared to WT cells (Figure 5G). Taken together, our findings demonstrate that
309 PTP1B-KO iNeutrophils are more responsive to *A. fumigatus* resulting in enhanced recruitment,
310 swarming and inhibition of fungal growth.

311

312 **Discussion**

313 iPSC-derived neutrophils can exert many classic primary neutrophil functions. In vivo mouse
314 studies using infusible iNeutrophils show promise for treating diseases ranging from bacterial infection
315 to cancer ^{4,6,25-27}. However, many of these iNeutrophils display inhibited or lower functional capacity
316 compared to primary human neutrophils ³⁻⁶. Therefore, there is a need to improve our understanding of
317 the molecular signaling pathways that regulate iNeutrophil function to enhance their use as a clinical
318 therapy. iNeutrophils can be genetically modified and thus are a valuable tool for dissecting pathways
319 regulating cell migration and antimicrobial response. In this study, we genetically manipulated
320 iNeutrophils and found that deletion of the phosphatase PTP1B increases cellular activation and motility
321 and improves key neutrophil antimicrobial effector functions.

322 PTP1B is a non-receptor tyrosine phosphatase that targets a variety of signaling pathways
323 including JAK/STAT, PI3K, and Ras/MAPK ¹⁷. Thus, PTP1B acts as an intracellular checkpoint to negatively
324 regulate cell responses. PTP1B has been targeted for dendritic cell and CAR T-cell based
325 immunotherapies, in which deletion enhanced cell activation and tumor cytotoxicity ^{28,29}. Additionally,
326 specific neutrophil effector functions including migration, phagocytosis, NETosis, and cytokine
327 production have been shown to be affected by PTP1B phosphatase activity ³⁰⁻³². Accordingly, we found
328 that deletion of PTP1B increased PI3K and MAPK signaling and improved iNeutrophil function.

329 Neutrophils are critical for clearance of fungal infections, including the opportunistic pathogen
330 *A. fumigatus*, which commonly infects immunosuppressed patients ³³. We found that PTP1B-KO
331 iNeutrophils are significantly better at inhibiting fungal growth over WT cells, due to enhanced
332 recruitment to *A. fumigatus*. PTP1B has been shown to regulate cell motility, but its activating versus
333 inhibitory effects are cell-type and chemokine dependent ^{15,16,32}. Here we show that deletion of PTP1B in
334 human iNeutrophils resulted in increased chemotaxis to fMLP. Furthermore, KO iNeutrophils showed
335 enhanced migration in the presence of the fungal pathogen *A. fumigatus*, likely in response to pathogen
336 associated molecular patterns (PAMPs). PTP1B directly targets p38 to inhibit MAPK signaling involved in
337 cell migration towards fMLP ³⁴. Indeed, MAPK signaling was increased in stimulated PTP1B-KO
338 iNeutrophils and may promote cell motility towards other stimuli including *A. fumigatus*. Additionally,
339 overexpression of PTP1B results in disorganized distribution of F-actin and focal adhesions ³⁵. We found
340 that PTP1B-KO iNeutrophils had increased phosphorylated HS1 and actin polymerization after fMLP
341 stimulation, as well as increased cell polarization in response to *A. fumigatus*. HS1 activates Rac-GTPase
342 signaling and Arp2/3-mediated actin polymerization necessary for cell polarity during chemotaxis ^{18,36}.
343 Thus, PTP1B may limit iNeutrophil motility through inhibition of MAPK signaling and actin organization.

344 During tissue damage and pathogen clearance, neutrophils produce chemotactic factors such as
345 IL-8 and LTB4 to amplify recruitment and promote swarming ^{37,38}. We and others have shown that
346 primary neutrophils cluster and produce IL-8 in response to *A. fumigatus* ^{13,39,40}, and addition of IL-8
347 alone can promote primary neutrophil swarming and inhibition of *A. fumigatus* growth ⁴⁰. Here we show
348 that PTP1B-KO iNeutrophils are significantly better at swarming fungal hyphae than WT cells. This is
349 likely due to increased production of IL-8, as this chemokine was elevated with Zymosan stimulation. WT
350 iNeutrophils are capable of swarming but do so infrequently due to limited recruitment to *A. fumigatus*.
351 We found no differences in expression of the LTB4 receptor BLT1R or LTB4 release after fMLP
352 stimulation in WT vs KO cells. Thus, the increased ability of PTP1B-KO iNeutrophils to swarm is likely due
353 to elevated inflammatory signaling initiated upon interaction with fungal hyphae.

354 Swarming can inhibit fungal growth through release of ROS, NETs and granule proteins such as
355 MPO ⁴¹. Drug inhibition of PTP1B in murine neutrophils reduces the capacity to NET ³². Here, we show
356 that deletion of PTP1B reduces iNeutrophil NET and ROS production in response to PMA stimulation.
357 Although, WT iNeutrophils were more responsive to PMA than KO iNeutrophils, the majority of cells
358 remained inactive in the presence of *A. fumigatus* and were not recruited to hyphae. The differential
359 response of WT iNeutrophils to these two stimuli is likely due to differences in receptor activation and
360 the potency of each stimulus. We predict that PTP1B-null iNeutrophils produce ROS and NETs in

361 response to *A. fumigatus* due to increased cell activation and recruitment to hyphae. Thus, increased
362 cell migration and swarming of PTP1B-KO iNeutrophils likely promotes release of ROS and NETs that are
363 responsible for inhibiting hyphal growth.

364 Neutrophil phagocytosis is a means for inhibiting fungal growth at the germling stage. PTP1B-
365 KO iNeutrophils readily phagocytosed *A. fumigatus* germlings, correlating to increased uptake of *E. coli*
366 coated beads. Increased actin polymerization in KO cells may promote phagocytosis as remodeling of
367 the actin cytoskeleton is necessary for formation of the phagosome (13). Enhanced TLR signaling may
368 also increase iNeutrophil phagocytosis. While, TLRs are not phagocytic receptors, they can prime
369 neutrophils to promote phagocytosis (32). Accordingly, in response to LPS or Zymosan treatment, we
370 found increased production of key inflammatory mediators, including IL-1 β and TNF α . Studies with
371 PTP1B-/ mice have shown increased TLR4 signaling in response to LPS stimulation^{30,42}, supporting the
372 idea that intracellular signaling is increased downstream of PRRs in PTP1B-KO iNeutrophils. Taken
373 together, PTP1B-null iNeutrophils are more responsive to *A. fumigatus* and are capable of inhibiting
374 fungal growth via recruitment and activation of antimicrobial functions including swarming,
375 phagocytosis, NETosis and ROS production.

376 A caveat of our experiments is the use of the total population of differentiated iNeutrophils. Our
377 flow cytometry analysis of lineage marker expression indicates that iNeutrophils are heterogeneous and
378 vary in their level of neutrophil maturation. In particular, PTP1B-KO iNeutrophils are less mature than
379 WT cells, with lower expression of CD15 and CD16. Immature neutrophils have reduced capacity for
380 NETosis and phagocytosis^{43,44}. Accordingly, we found decreased NET and ROS production in response to
381 PMA stimulation by the total population of PTP1B-KO iNeutrophils. To normalize the maturity level
382 between WT and KO iNeutrophils, we used CD15-positive magnetic bead selection, but saw no
383 improvement in these antimicrobial functions by PTP1B-KO iNeutrophils (data not shown). Thus, the
384 decrease in NETosis and ROS production is likely due to the impact of PTP1B on downstream signaling
385 and not differences in neutrophil maturity. In flow cytometry assays, we can dissect differences in
386 PTP1B-regulated function versus neutrophil maturity by gating on mature neutrophils (CD15+CD16+)
387 only. Through this method, we identified enhanced phagocytosis within mature PTP1B-KO iNeutrophils,
388 but not the bulk population (data not shown). We are currently evaluating methods to generate a more
389 homogenous population of mature PTP1B-KO iNeutrophils.

390 Here, we identified PTP1B as a negative regulator of iPSC-derived neutrophil cellular activation
391 and effector function. Upon deletion of this phosphatase, we found enhanced intracellular signaling and
392 iNeutrophil function. Our findings suggest that inhibition of PTP1B may be a promising target for further
393 development of iNeutrophil therapies for neutropenic patients with bacterial and fungal infections.

394

395 **Data Sharing Statement**

396 All relevant data are included in the manuscript.

397

398 **Acknowledgements**

399 Research reported in this publication was supported by the National Institute of Allergy and Infectious
400 Diseases (NIAID) of the National Institutes of Health under Award Number RO1 AI134749-05 and
401 T32AI055397. The content is solely the responsibility of the authors and does not necessarily represent
402 the official views of the NIH. The funders had no role in study design, data collection and analysis,
403 decision to publish, or preparation of the manuscript. The content is solely the responsibility of the
404 authors and does not necessarily represent the official views of the National Institutes of Health.

405

406 **Contribution:** M.A.G., D.A.B., T.J.S., A.N.P., and H.S.J., performed experiments. M.A.G. D.A.B., T.J.S.,
407 A.N.P., J.B., H.Q.D., I.I.S., and A.H. analyzed and interpreted data. M.A.G. and A.H. designed the research
408 and wrote the paper.

409 **Conflict-of-interest disclosure:** I.I.S. serves on Scientific Advisory Board of Umoja Biopharma.

410 **Correspondence:** Anna Huttenlocher, University of Wisconsin–Madison, 1550 Linden Dr, Room 4225,
411 Madison, WI 53706; e-mail: huttenlocher@wisc.edu

412

413

414 **References**

- 415 1. Marfin AA, Price TH. Granulocyte transfusion therapy. *J Intensive Care Med*. Feb 2015;30(2):79-
416 88. doi:10.1177/0885066613498045
- 417 2. Cohen T, Simmons SC, Pham HP, Staley EM. Granulocyte Transfusion: Clinical Updates and a
418 Practical Approach to Transfusion. *Clin Lab Med*. Dec 2021;41(4):647-657. doi:10.1016/j.cll.2021.07.007
- 419 3. Lachmann N, Ackermann M, Frenzel E, et al. Large-scale hematopoietic differentiation of human
420 induced pluripotent stem cells provides granulocytes or macrophages for cell replacement therapies.
Stem Cell Reports. Feb 10 2015;4(2):282-96. doi:10.1016/j.stemcr.2015.01.005
- 421 4. Miyauchi M, Ito Y, Nakahara F, et al. Efficient production of human neutrophils from iPSCs that
422 prevent murine lethal infection with immune cell recruitment. *Blood*. Dec 16 2021;138(24):2555-2569.
423 doi:10.1182/blood.2021011576
- 424 5. Brok-Volchanskaya VS, Bennin DA, Suknuntha K, Klemm LC, Huttenlocher A, Slukvin I. Effective
425 and Rapid Generation of Functional Neutrophils from Induced Pluripotent Stem Cells Using ETV2-
426 Modified mRNA. *Stem Cell Reports*. Dec 10 2019;13(6):1099-1110. doi:10.1016/j.stemcr.2019.10.007
- 427 6. Trump LR, Nayak RC, Singh AK, et al. Neutrophils Derived from Genetically Modified Human
428 Induced Pluripotent Stem Cells Circulate and Phagocytose Bacteria In Vivo. *Stem Cells Transl Med*. Jun
429 2019;8(6):557-567. doi:10.1002/sctm.18-0255
- 430 7. Azcutia V, Parkos CA, Brazil JC. Role of negative regulation of immune signaling pathways in
431 neutrophil function. *J Leukoc Biol*. Dec 19 2017;doi:10.1002/JLB.3MIR0917-374R
- 432 8. Majumder A, Suknuntha K, Bennin D, et al. Generation of Human Neutrophils from Induced
433 Pluripotent Stem Cells in Chemically Defined Conditions Using ETV2 Modified mRNA. *STAR Protoc*. Sep
434 18 2020;1(2)doi:10.1016/j.xpro.2020.100075
- 435 9. Nowicka M, Krieg C, Crowell HL, et al. CyTOF workflow: differential discovery in high-throughput
436 high-dimensional cytometry datasets. *F1000Res*. 2017;6:748. doi:10.12688/f1000research.11622.3
- 437 10. Yamahashi Y, Cavnar PJ, Hind LE, et al. Integrin associated proteins differentially regulate
438 neutrophil polarity and directed migration in 2D and 3D. *Biomed Microdevices*. Oct 2015;17(5):100.
439 doi:10.1007/s10544-015-9998-x
- 440 11. Warrick JW, Timm A, Swick A, Yin J. Tools for Single-Cell Kinetic Analysis of Virus-Host
441 Interactions. *PLoS One*. 2016;11(1):e0145081. doi:10.1371/journal.pone.0145081
- 442 12. Livak KJ, Schmittgen TD. Analysis of relative gene expression data using real-time quantitative
443 PCR and the 2(-Delta Delta C(T)) Method. *Methods*. Dec 2001;25(4):402-8. doi:10.1006/meth.2001.1262
- 444 13. Schoen TJ, Calise DG, Bok JW, et al. *Aspergillus fumigatus* transcription factor ZfpA regulates
445 hyphal development and alters susceptibility to antifungals and neutrophil killing during infection. *PLoS*
446 *Pathog*. May 2023;19(5):e1011152. doi:10.1371/journal.ppat.1011152
- 447

448 14. Heinonen KM, Dube N, Bourdeau A, Lapp WS, Tremblay ML. Protein tyrosine phosphatase 1B
449 negatively regulates macrophage development through CSF-1 signaling. *Proc Natl Acad Sci U S A*. Feb 21
450 2006;103(8):2776-81. doi:10.1073/pnas.0508563103

451 15. Cortesio CL, Chan KT, Perrin BJ, et al. Calpain 2 and PTP1B function in a novel pathway with Src
452 to regulate invadopodia dynamics and breast cancer cell invasion. *J Cell Biol*. Mar 10 2008;180(5):957-
453 71. doi:10.1083/jcb.200708048

454 16. Arregui CO, Gonzalez A, Burdisso JE, Gonzalez Wusener AE. Protein tyrosine phosphatase PTP1B
455 in cell adhesion and migration. *Cell Adh Migr*. Sep-Oct 2013;7(5):418-23. doi:10.4161/cam.26375

456 17. Villamar-Cruz O, Loza-Mejia MA, Arias-Romero LE, Camacho-Arroyo I. Recent advances in PTP1B
457 signaling in metabolism and cancer. *Biosci Rep*. Nov 26 2021;41(11)doi:10.1042/BSR20211994

458 18. Cavnar PJ, Mogen K, Berthier E, Beebe DJ, Huttenlocher A. The actin regulatory protein HS1
459 interacts with Arp2/3 and mediates efficient neutrophil chemotaxis. *J Biol Chem*. Jul 20
460 2012;287(30):25466-77. doi:10.1074/jbc.M112.364562

461 19. Berthier E, Surfus J, Verbsky J, Huttenlocher A, Beebe D. An arrayed high-content chemotaxis
462 assay for patient diagnosis. *Integr Biol (Camb)*. Nov 2010;2(11-12):630-8. doi:10.1039/c0ib00030b

463 20. Hind LE, Vincent WJ, Huttenlocher A. Leading from the Back: The Role of the Uropod in
464 Neutrophil Polarization and Migration. *Dev Cell*. Jul 25 2016;38(2):161-9.
465 doi:10.1016/j.devcel.2016.06.031

466 21. May RC, Machesky LM. Phagocytosis and the actin cytoskeleton. *J Cell Sci*. Mar 2001;114(Pt
467 6):1061-77. doi:10.1242/jcs.114.6.1061

468 22. Papayannopoulos V. Neutrophil extracellular traps in immunity and disease. *Nat Rev Immunol*.
469 Feb 2018;18(2):134-147. doi:10.1038/nri.2017.105

470 23. Li D, Wu M. Pattern recognition receptors in health and diseases. *Signal Transduct Target Ther*.
471 Aug 4 2021;6(1):291. doi:10.1038/s41392-021-00687-0

472 24. Kienle K, Lammermann T. Neutrophil swarming: an essential process of the neutrophil tissue
473 response. *Immunol Rev*. Sep 2016;273(1):76-93. doi:10.1111/imr.12458

474 25. Chang Y, Syahirah R, Wang X, et al. Engineering chimeric antigen receptor neutrophils from
475 human pluripotent stem cells for targeted cancer immunotherapy. *Cell Rep*. Jul 19 2022;40(3):111128.
476 doi:10.1016/j.celrep.2022.111128

477 26. Chang Y, Cai X, Syahirah R, et al. CAR-neutrophil mediated delivery of tumor-microenvironment
478 responsive nanodrugs for glioblastoma chemo-immunotherapy. *Nat Commun*. Apr 20 2023;14(1):2266.
479 doi:10.1038/s41467-023-37872-4

480 27. Harris JD, Chang Y, Syahirah R, Lian XL, Deng Q, Bao X. Engineered anti-prostate cancer CAR-
481 neutrophils from human pluripotent stem cells. *J Immunol Regen Med*. May
482 2023;20doi:10.1016/j.regen.2023.100074

483 28. Penafuerte C, Feldhamer M, Mills JR, et al. Downregulation of PTP1B and TC-PTP
484 phosphatases potentiate dendritic cell-based immunotherapy through IL-12/IFNgamma signaling.
485 *Oncoimmunology*. 2017;6(6):e1321185. doi:10.1080/2162402X.2017.1321185

486 29. Wiede F, Lu KH, Du X, et al. PTP1B Is an Intracellular Checkpoint that Limits T-cell and CAR T-cell
487 Antitumor Immunity. *Cancer Discov*. Mar 1 2022;12(3):752-773. doi:10.1158/2159-8290.CD-21-0694

488 30. Yue L, Xie Z, Li H, et al. Protein Tyrosine Phosphatase-1B Negatively Impacts Host Defense
489 against *Pseudomonas aeruginosa* Infection. *Am J Pathol*. May 2016;186(5):1234-44.
490 doi:10.1016/j.ajpath.2016.01.005

491 31. Yue L, Yan M, Tremblay ML, et al. PTP1B negatively regulates nitric oxide-mediated
492 *Pseudomonas aeruginosa* killing by neutrophils. *PLoS One*. 2019;14(9):e0222753.
493 doi:10.1371/journal.pone.0222753

494 32. Song D, Adrover JM, Felice C, et al. PTP1B inhibitors protect against acute lung injury and
495 regulate CXCR4 signaling in neutrophils. *JCI Insight*. Jul 22 2022;7(14)doi:10.1172/jci.insight.158199

496 33. Lionakis MS, Drummond RA, Hohl TM. Immune responses to human fungal pathogens and
497 therapeutic prospects. *Nat Rev Immunol.* Jan 4 2023;1-20. doi:10.1038/s41577-022-00826-w

498 34. Medgyesi D, Hobeika E, Biesen R, et al. The protein tyrosine phosphatase PTP1B is a negative
499 regulator of CD40 and BAFF-R signaling and controls B cell autoimmunity. *J Exp Med.* Mar 10
500 2014;211(3):427-40. doi:10.1084/jem.20131196

501 35. Liu F, Sells MA, Chernoff J. Protein tyrosine phosphatase 1B negatively regulates integrin
502 signaling. *Curr Biol.* Jan 29 1998;8(3):173-6. doi:10.1016/s0960-9822(98)70066-1

503 36. Weiner OD, Servant G, Welch MD, Mitchison TJ, Sedat JW, Bourne HR. Spatial control of actin
504 polymerization during neutrophil chemotaxis. *Nat Cell Biol.* Jun 1999;1(2):75-81. doi:10.1038/10042

505 37. de Oliveira S, Rosowski EE, Huttenlocher A. Neutrophil migration in infection and wound repair:
506 going forward in reverse. *Nat Rev Immunol.* May 27 2016;16(6):378-91. doi:10.1038/nri.2016.49

507 38. Snarr BD, Qureshi ST, Sheppard DC. Immune Recognition of Fungal Polysaccharides. *J Fungi*
508 (*Basel*). Aug 28 2017;3(3)doi:10.3390/jof3030047

509 39. Hind LE, Giese MA, Schoen TJ, Beebe DJ, Keller N, Huttenlocher A. Immune Cell Paracrine
510 Signaling Drives the Neutrophil Response to *A. fumigatus* in an Infection-on-a-Chip Model. *Cell Mol*
511 *Bioeng.* Apr 2021;14(2):133-145. doi:10.1007/s12195-020-00655-8

512 40. Jones CN, Dimisko L, Forrest K, et al. Human Neutrophils Are Primed by Chemoattractant
513 Gradients for Blocking the Growth of *Aspergillus fumigatus*. *J Infect Dis.* Feb 1 2016;213(3):465-75.
514 doi:10.1093/infdis/jiv419

515 41. Hopke A, Scherer A, Kreuzburg S, et al. Publisher Correction: Neutrophil swarming delays the
516 growth of clusters of pathogenic fungi. *Nat Commun.* May 14 2020;11(1):2492. doi:10.1038/s41467-020-
517 16446-8

518 42. Xu H, An H, Hou J, et al. Phosphatase PTP1B negatively regulates MyD88- and TRIF-dependent
519 proinflammatory cytokine and type I interferon production in TLR-triggered macrophages. *Mol Immunol.*
520 Aug 2008;45(13):3545-52. doi:10.1016/j.molimm.2008.05.006

521 43. Wang L, Ai Z, Khoiratty T, et al. ROS-producing immature neutrophils in giant cell arteritis are
522 linked to vascular pathologies. *JCI Insight.* Oct 15 2020;5(20)doi:10.1172/jci.insight.139163

523 44. Montaldo E, Lusito E, Bianchessi V, et al. Cellular and transcriptional dynamics of human
524 neutrophils at steady state and upon stress. *Nat Immunol.* Oct 2022;23(10):1470-1483.
525 doi:10.1038/s41590-022-01311-1

526

527 **Figure Legends**

528 **Figure 1. Generation of PTP1B-KO iPSC-derived neutrophils.**

529 (A) Diagram illustrates sgRNAs targeting exon 3 of *PTPN1* for CRISPR/Cas9 mediated deletion of a 67bp
530 region at the stem cell stage. (B) Timeline for neutrophil differentiation from bone marrow derived
531 iPSCs. (C) Western blot confirmation of PTP1B CRISPR/Cas9 mediated deletion in differentiated
532 neutrophils. (D) Representative cytopsins showing morphological confirmation of neutrophil
533 differentiation. (E) Flow cytometry staining of differentiated neutrophils and myeloid cells. Cells were
534 gated on live cells. (F) Histogram plots of normalized flow cytometry surface receptor expression data in
535 (E). Data were normalized individually to each fluorescent marker and presents the range of expression.
536 (G) Cell viability of iPSC-derived neutrophils compared to human peripheral blood (PB) neutrophils.
537 Diagram (B) was created with BioRender.com. Experiments were conducted at least three times, or as
538 indicated on the plot. Dots in (E) represent independent replicates and dots in (G) represent the average
539 of all replicates. Means \pm SEM are shown. *p* values were calculated by paired Student's t-test (E) or by
540 simple linear regression (G). *, *p* < 0.05; **, *p* < 0.01

541

542 **Figure 2. Deletion of PTP1B promotes intracellular signaling, motility and actin polymerization.**

543

544 (A) Representative western blots and quantification (B) of ERK, HS1, AKT phospho-signaling after
545 stimulation with 1uM fMLP for 3 minutes. (C) iNeutrophil chemotactic index and mean velocity in
546 response to an fMLP gradient over 45 minutes of imaging. (D) Representative track plots of cells
547 migrating in response to an fMLP gradient. Blue tracks indicate cells that traveled towards the fMLP
548 source, whereas red tracks indicate cells that moved away. (E) Representative immunofluorescence
549 images of F-actin staining after 100nM fMLP stim. (F) Quantified integrated density of F-actin staining.
550 Dots represent individual cells. WT n=50, KO n=56. Scale bar represents 20 μ m. Experiments were
551 conducted at least three times, or as indicated on the plot. Dots in (B, C) represent independent
552 replicates. Bars in (B, C) represent means \pm SEM. Bars in (F) represent LSmeans \pm SEM. p values were
553 calculated by One-sample t-test (B), unpaired Student's t-test (C) or ANOVA with Tukey's multiple
554 comparisons (F). *, p < 0.05; **, p < 0.01; ****, p < 0.0001.

555

556 **Figure 3. Deletion of PTP1B improves neutrophil phagocytosis but decreases production of ROS and
557 NETs.**

558 (A) iNeutrophil phagocytosis of acidified pHrodo *E. coli* beads quantified by flow cytometry. Percent
559 pHrodo+ cells of CD11b+CD15+ neutrophils or CD11b+CD15+CD16+ mature neutrophils. (B)
560 Quantification of iNeutrophil intracellular ROS production over time using DHR123 peroxynitrite
561 indicator following stimulation with 50ng/mL PMA. (C) NETosis quantified with Sytox Green DNA
562 indicator after 4 hour stimulation with 100ng/mL PMA. Experiments were conducted at least three
563 times, or as indicated on the plot. Dots in (A, C) represent independent replicates and dots in (B)
564 represent the average of all replicates. Means \pm SEM are shown. p values were calculated by paired
565 Student's t-test (A), simple linear regression (B), or One-sample t-test (C). *, p < 0.05; **, p < 0.001;
566 ****, p < 0.0001.

567

568 **Figure 4. Deletion of PTP1B increases inflammatory cytokine production.**

569 (A-D) Inflammatory cytokines produced by unstimulated iNeutrophils or after stimulation with
570 200ng/mL LPS or 10ug/mL Zymosan for 4 hours. Experiments were conducted three times. Dots
571 represent independent replicates. Means \pm SEM are shown. p values were calculated by paired
572 Student's t-test (A-D). *, p < 0.05.

573

574 **Figure 5. Deletion of PTP1B increases iNeutrophil swarming and inhibition of fungal growth.**

575 (A) Representative bright-field images of *A. fumigatus* co-culture with WT or PTP1B-KO iNeutrophils over
576 the course of 8 hours. Black arrows indicate germlings. White arrows indicate a phagocytosed germling.
577 Asterisks indicate iNeutrophil swarming and cluster formation. (B) Higher magnification bright-field
578 images of WT or PTP1B-KO iNeutrophil cell morphology and interaction with *A. fumigatus* hyphae.
579 Individual cells are outlined. (C) Quantification of iNeutrophil cell shape (circularity) at 0 and 4 hours of
580 co-incubation. Dots represent individual cells. WT n=414, KO n=396. (D) Representative time lapse
581 images of PTP1B-KO iNeutrophils phagocytosing and clustering around *A. fumigatus* hyphae. Black
582 arrows indicate germlings. White arrows indicate a phagocytosed germling. Asterisks indicate
583 iNeutrophil swarming and cluster formation. Clusters are outlined. (E) Quantification of percent of *A.*
584 *fumigatus* germlings surrounded by iNeutrophil clusters at 0, 1, 2, and 4 hours of co-incubation. (F)

585 Quantification of iNeutrophil cluster size at 0, 1, 2, and 4 hours of co-incubation. (G) Quantification of
586 hyphal length at 0 and 4 hours of co-culture with WT or PTP1B-KO iNeutrophils. Dots represent
587 individual germlings. WT n=138, KO n=110. Scale bars represent 50 μ m. Experiments were conducted at
588 least three times, or as indicated on the plot. Bars in (C,G) represent LSmeans \pm SEM. Dots in (E, F)
589 represent the mean \pm SEM. p values were calculated by ANOVA with Tukey's multiple comparisons (C,
590 G), linear regression (E), or paired Student's t-test (F) on the calculated area under the curve (AUC) for
591 each replicate. **, p < 0.01; ****, p < 0.0001.

Figure 5. Deletion of PTP1B increases iNeutrophil swarming and inhibition of fungal growth

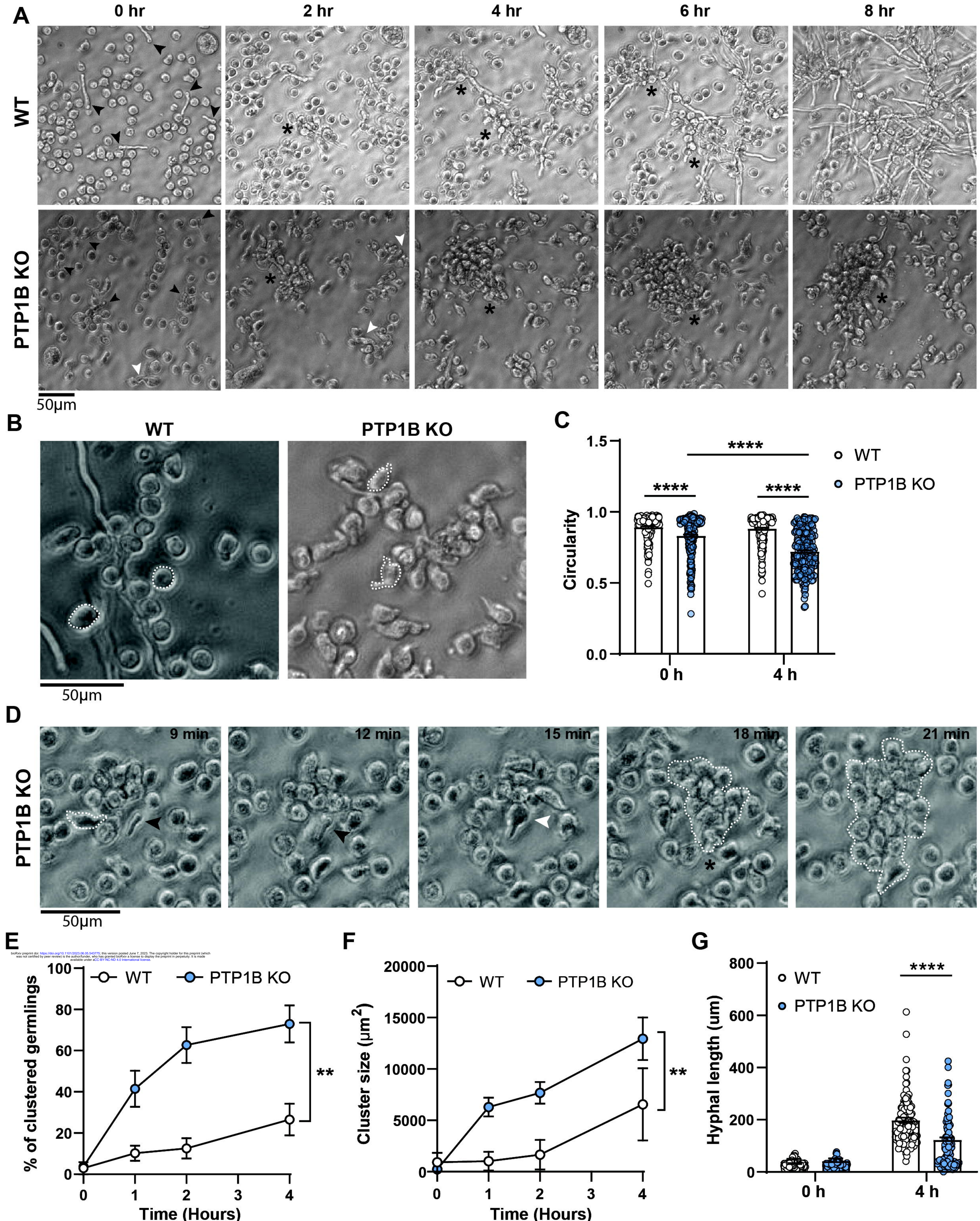


Figure 4. Deletion of PTP1B increases inflammatory cytokine production

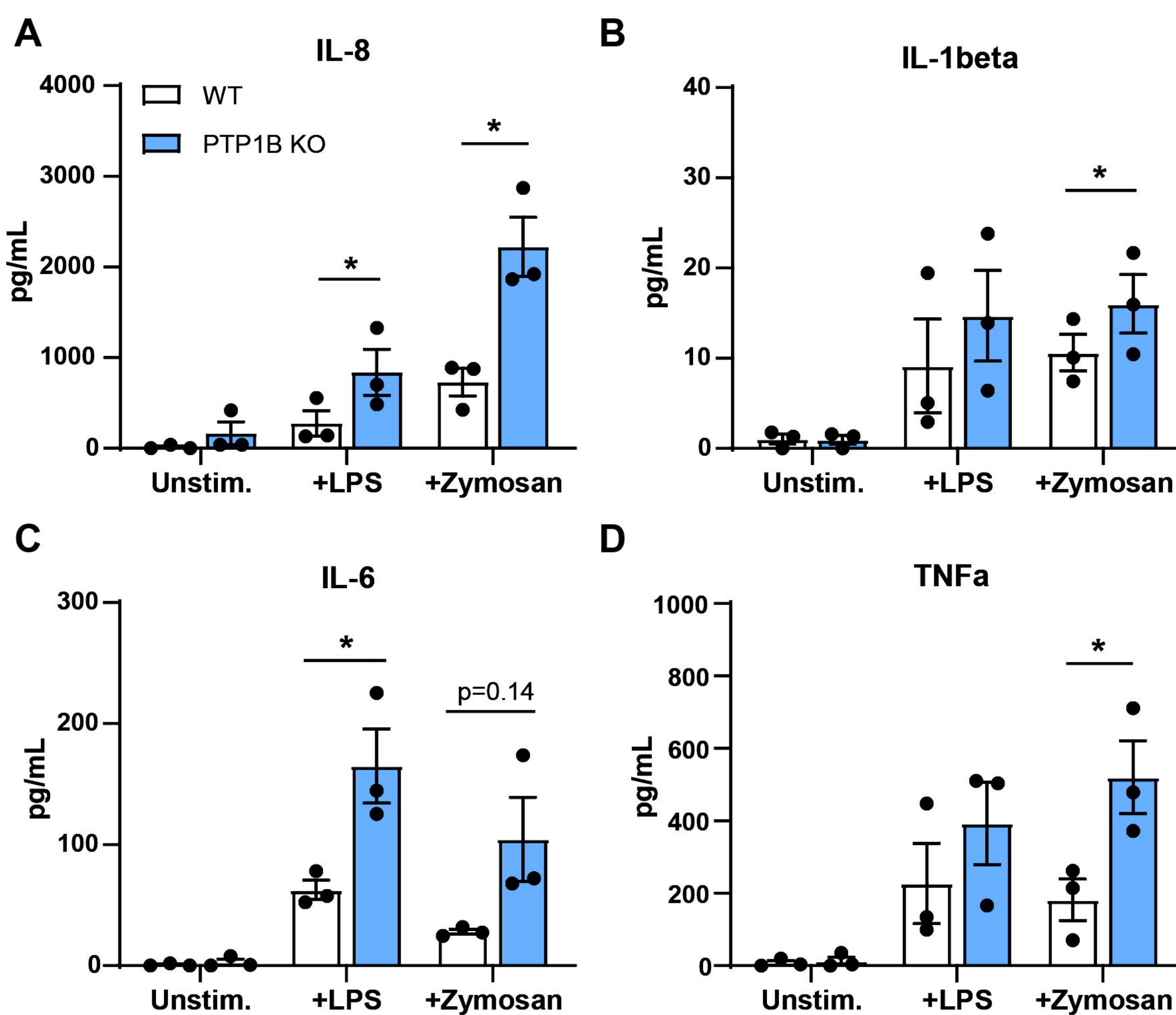


Figure 3. Deletion of PTP1B improves neutrophil phagocytosis, but decreases production of ROS and NETs

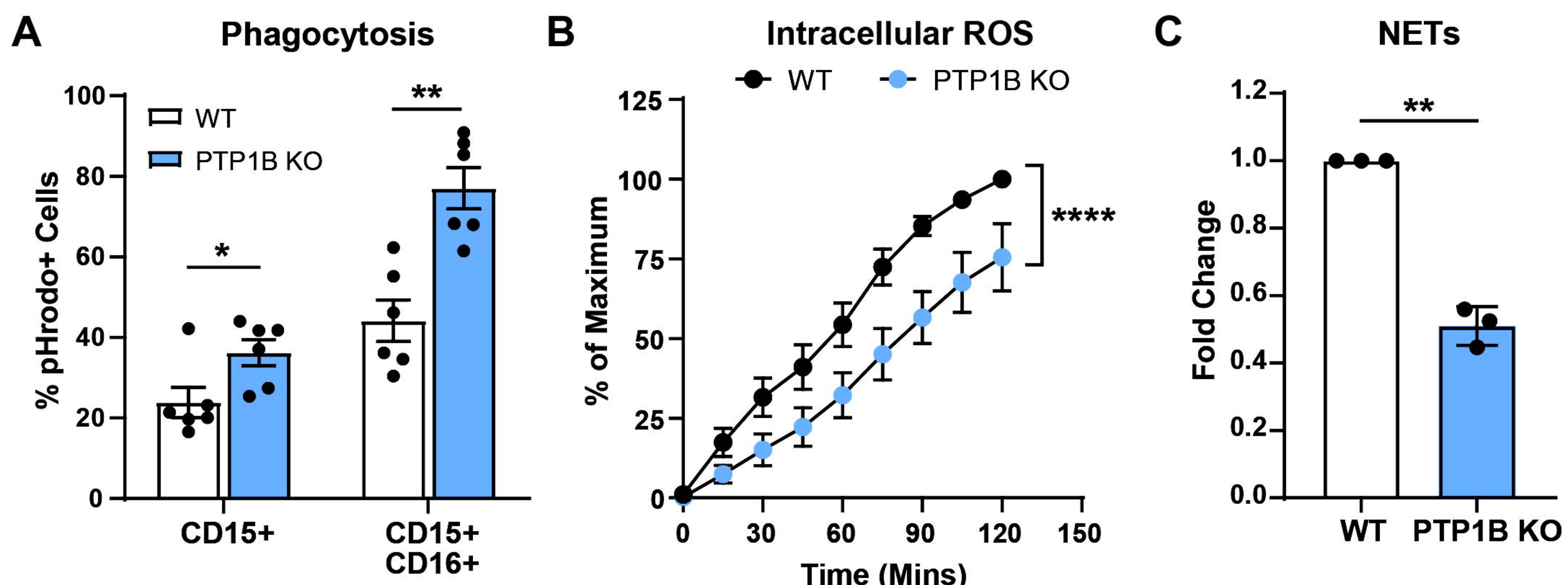


Figure 2. Deletion of PTP1B promotes intracellular signaling, motility, and actin polarization

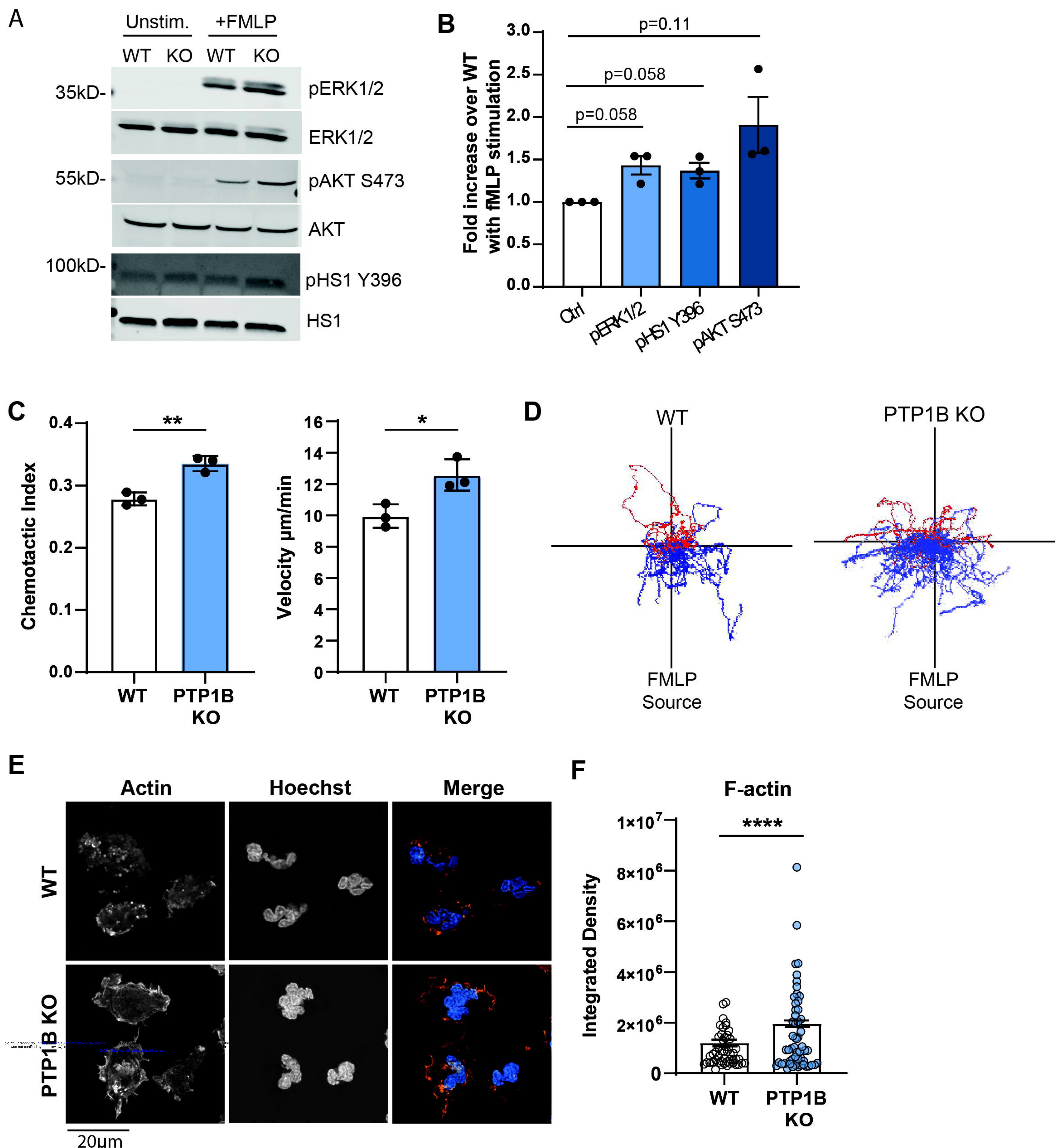


Figure 1. Generation of PTP1B-null iPSC-derived neutrophils

